Supporting Table S1.

Histogram Statistics for Model Metrics

	Relative Error		Coefficient of Variance		
	6-shell	8-shell	5-shell	6-shell	8-shell
TR	0.110	0.332	165.057	165.553	170.352
FA	0.037	0.133	187.409	189.392	192.558
RTOP	0.035	0.077	159.704	175.652	847.549
PA	0.106	0.159	163.669	160.874	160.072
KMEAN	0.188	0.137	162.137	166.965	188.512
KFA	1.296	2.428	177.794	161.878	156.807
ODI	0.272	0.309	172.030	185.796	186.440
VIC	0.108	0.040	164.887	170.468	169.658

Supporting Table S1. Quantitative comparisons of histogram features are shown to demonstrate the effects of DWI sampling scheme. Relative error values are given to compare the differences in metric values obtained with greater DWI sampling from those generated by the 5-shell set. Coefficient of Variance values are given as a measure of variability relative to the mean for scalar metrics obtained for each DWI sampling scheme.

Supporting Figure S2.

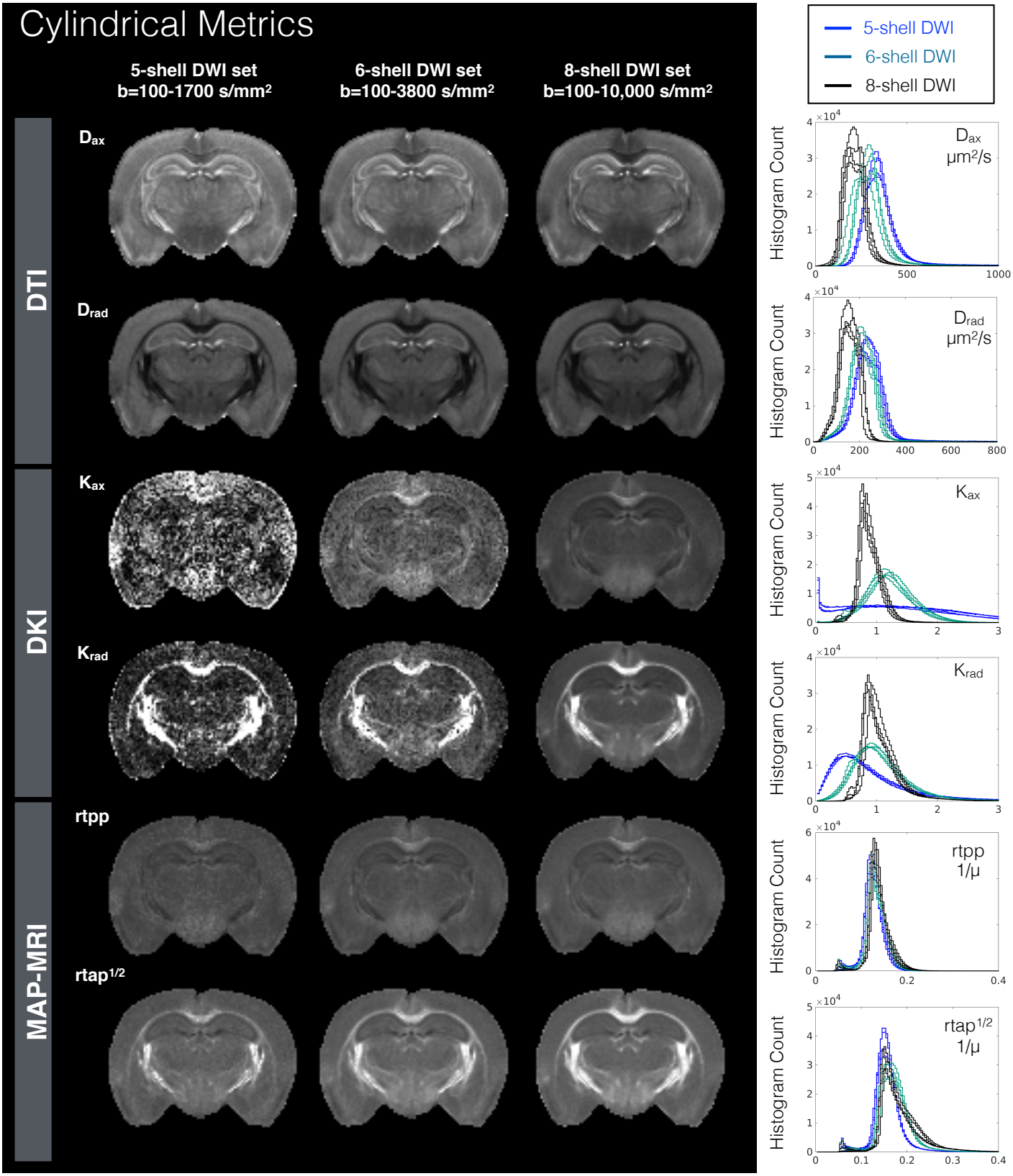

Supporting Figure S2. Metric maps and histograms to probe water movement along the primary eigenvector (Dax, Kax and rtpp) and perpendicular to it (Drad, Krad and rtap). DTI, DKI and MAP-MRI models were fit using diffusion weighted data from three sampling schemes having 5, 6 and 8 shells and density histogram plots (right column) for each metric in 4 mouse brain samples show the distribution of metric values. Metric map abbreviations: D_{ax}= axial diffusivity, D_{rad}= radial diffusivity, K_{ax}= axial kurtosis, K_{rad}= radial kurtosis, rtpp - return to the plane probability, rtpp - return to the axis probability.

Supporting Figure S3.

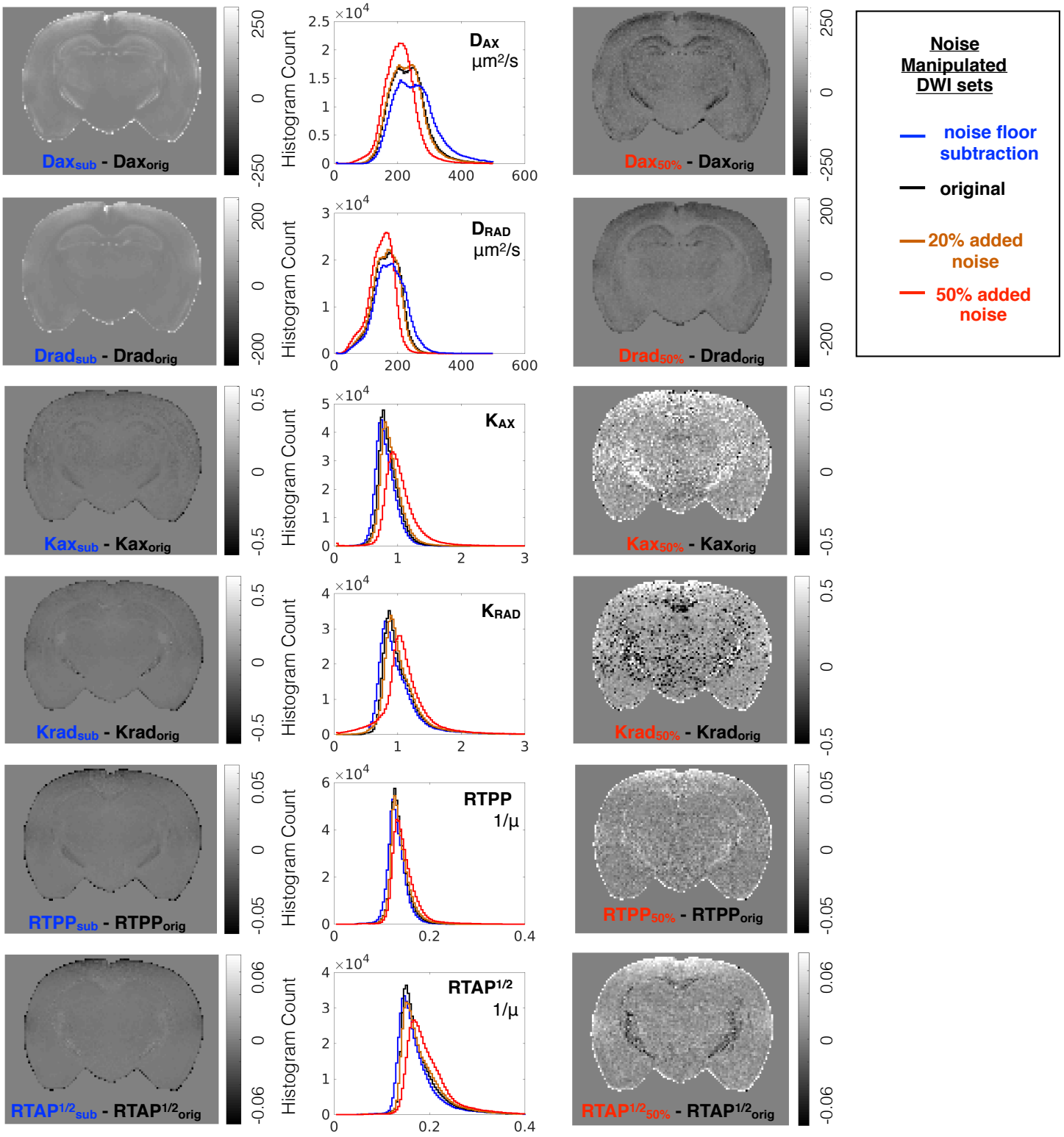

Supporting Figure S3. The effects of signal transformation and added noise are shown for metric maps for cylindrical components from the DTI, DKI and MAP models. For each metric, whole brain histograms are shown for modeling of the original DWI data set (black) and of the same data set following noise floor subtraction (blue), addition of 20% or 50% rectified noise (orange and red respectively). To visualize the localization of metric differences resulting from noise manipulation, difference maps are shown for the same slice.

Supporting Figure S4.

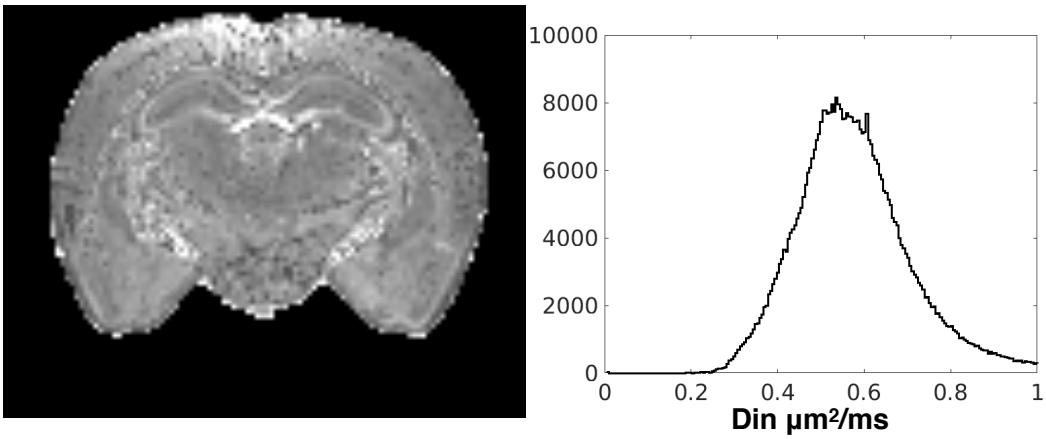

Supporting Figure S4. Interstitial diffusivity (D_{IN}) as a free parameter. The NODDI made was fit with D_{IN} left as a free parameter and the scalar image (left) and histogram of values are shown in this figure. Notably D_{IN} spans a range of values and appears to demonstrate some dependence on tissue type.

Supporting Figure S5.

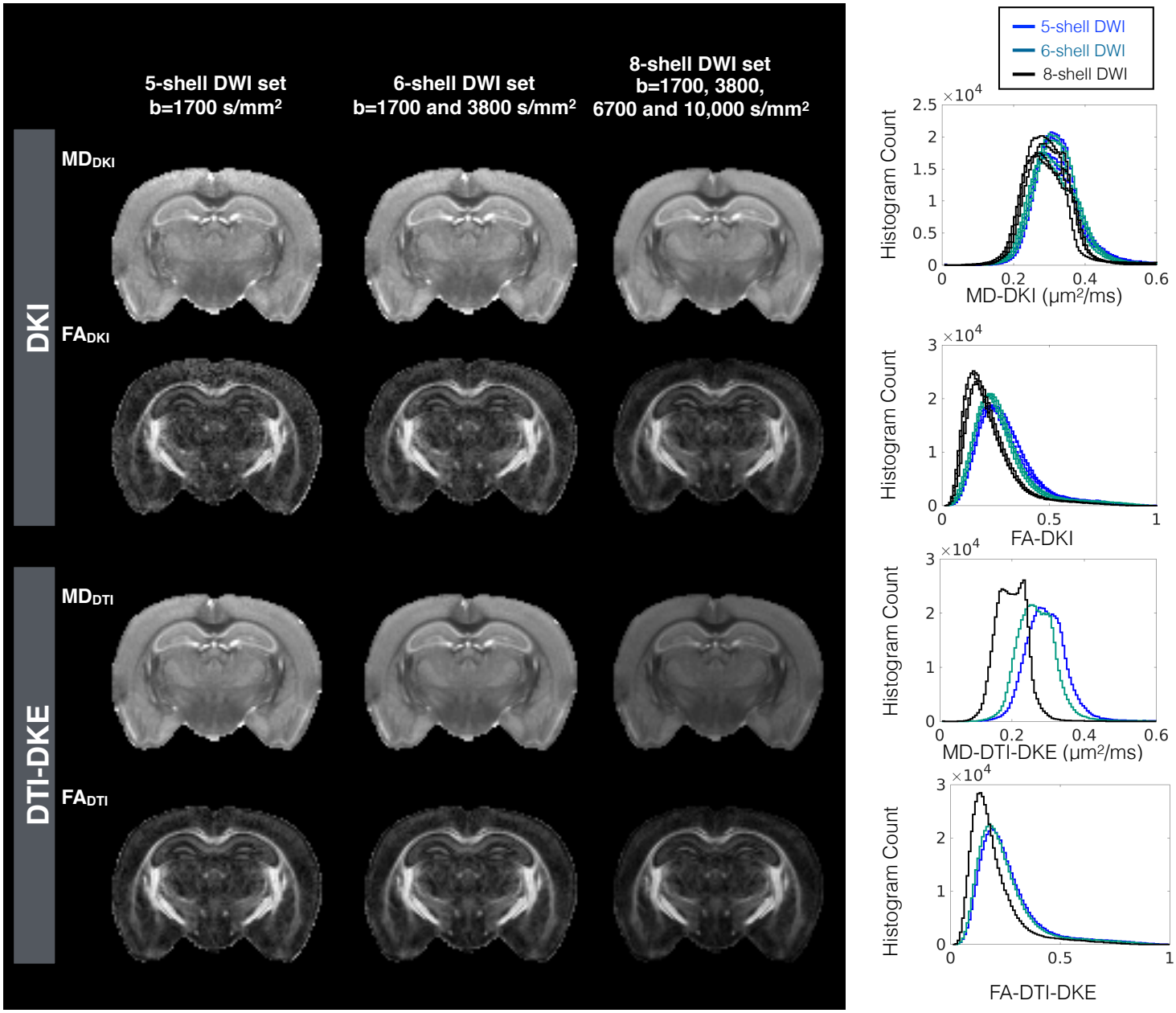

Supporting Figure S5. The effects of DWI sampling scheme on DTI metrics derived from the DKI model (MD-DKI and FA-DKI) or from the DTI model using the DKE implementation (MD-DTI-DKE and FA-DTI-DKE). The MD maps and histogram mode and shape are relatively stable across the full range of DWI sampling schemes when estimated from the DKI model, but demonstrate DWI sampling dependence when estimated from the DTI model alone.